S. Afr. J. Chem., 2014, **67**, 160–166,
<http://journals.sabinet.co.za/sajchem/>.

Quininium Malates: Partial Chiral Discrimination *via* Diastereomeric Salt Formation

Nikoletta B. Báthori*, Ayesha Jacobs, Luigi R. Nassimbeni and Baganetsi K. Sebogisi

Crystal Engineering Research Unit, Department of Chemistry, Cape Peninsula University of Technology, P.O. Box 652, Cape Town, 8000, South Africa.

Received 22 July 2014, revised 16 September 2014, accepted 16 September 2014.

ABSTRACT

Quinine was employed as a resolving agent for racemic malic acid. The resultant product was a quininium salt containing 75 % of the *D*-malate anion. Quinine was also crystallized with pure *L*- and *D*-malic acids and the structures of the resulting diastereomeric salts were elucidated. The crystal packings were analyzed in terms of their non-bonded interactions and the conformation of the quinine, which was compared with other quinine structures recorded in the Cambridge Structural Database. The results indicate that the mechanism of enantiomeric resolution is reliant upon hydrogen bonded interactions.

KEYWORDS

Chiral discrimination, diastereomeric salt, quinine.

1. Introduction

Selectivity arises from the phenomenon of molecular recognition and depends on such factors as complementarity of binding sites, the strengths of the relevant non-bonding interactions and the conformational adaptability of the host molecule.

The most demanding form of separation is that of enantiomeric resolution. This is because the physical properties of the (*R*)- and (*S*)-forms of the two optical isomers have identical properties such as melting point, boiling point, vapour pressure, density and differ only in their reactions toward chiral compounds and polarized light. The enantiomeric purity of a compound is important in the analytical, food, pesticide and particularly in the pharmaceutical industries. Resolution of racemic modifications of organic molecules is of considerable importance to the pharmaceutical industry hence these compounds represents close to *ca.* 30 % of all drug sales worldwide.[1] The global pharma market in 2012 was 990 billion USD and a recent estimate of the sale of single-enantiomer drugs is of the order of 300 billion USD.[2] When a compound is produced as a racemic modification in certain cases only one of the enantiomers exhibits the required biological effect. Different techniques are used to separate the enantiomers, such as spontaneous resolution by crystallization, enzymatic transformations, and chromatographic methods. Diastereomeric salt formation is also a well-known and widely used technique and a typical method employed in the separation of racemic modifications of carboxylic acids and amines.[3]

Quinine, the major component of the cinchona alkaloids has a long history as a resolving agent. Pasteur employed its derivative quinicine to resolve tartaric acid.[4] Kozma's review of resolutions *via* diastereomeric salt formation catalogues 352 resolution experiments with quinine, mostly of carboxylic acids, but also lists ketones and alcohols.[5] However, relatively few crystal structures of diastereomeric salts have been reported as a recent Cambridge Structural Database[6] (CSD, version 5.35, 2014 May) search conducted with ConQuest[7]. Two of the publications discuss a crystal structure, which contains quinine in a neutral form[8] while the majority of the work describes crystal structures in which the quinine moiety is protonated. The salt formation ability of quinine was investigated by exposing quinine to achiral compounds, such as salicylic acid and saccharin.[9] In addition a series of chiral diastereomeric salts of quinine were synthesized and their structures were discussed, such as diquinine biphenyl-2,2′-dicarboxylic acid monohydrate (CSD code JIFYOM).[10] Quinine was used also to assign the absolute configuration for the building block of a β-peptide oligomer, *trans*-2-aminocyclohexanecarboxylic acid (LIVWOC[11]) and a series of products tested to inhibit renal dipeptidase ((–) quininium (+)-2,2-dimethylcyclopropanecarboxylate monohydrate, FIJSUM12[12]). Surprisingly, very few structural data are available from resolution experiments conducted with quinine. A racemic modification of [fluoro(hydroxyphenylphosphinyl)methyl]-phosphonic acid was crystallized with quinine and the 98 % diastereomerically pure diquinine salt was obtained (YUKMOG[13]). Quinine was used also to resolve (±)-hydroazulenone, the starting material for the total synthesis of sesquiterpenoids (FEQZEG[14]), enriching enantiomers during the preparation of paracyclophen phosphine ligands (BEYTIJ[15]) and resolving 1,1′-binaphtyl-2,2′-dicarboxylic acid *via* diastereomeric salt formation (URIJAV[16]).

A study of chiral discrimination of mandelic acid by quinine was investigated *via* a series of competition experiments, in which the mole fraction of (*R*)-mandelic acid was varied systematically from 0 to 1. The experiment yielded a selectivity curve. The concomitant structures of the quininium mandelates were elucidated and it was concluded that the asymmetric unit containing (*R*)-, (*R*)- and (*S*)-mandelate salt of quinine dominates over a wide range of the selectivity curve.[17]). The naturally occurring isomer of malic acid is the *L*(+) form and is found in apples and many other fruits and plants. Its metabolism is well understood, but little is known about the fate of *D*-(-)-malic acid in the body.[18] Attempted separation of the two forms was carried out previously by exposing the racemic malic acid to *L*-citrulline (SACSOE[19]) and *R*-phenylethylamine (EYOBAV[20]).

We now present the structures of the salts, which arise, from the combination of quinine (QUIN) with *L*, *D* and racemic (*DL*) malic acid (MA). Four structures were elucidated, namely **1**:

* To whom correspondence should be addressed. E-mail: bathorin@cput.ac.za

$2(QUIN^{+})\cdot(L\text{-}MA^{2-})\cdot 2H_2O$, **2**: $2(QUIN^{+})\cdot(D\text{-}MA^{2-})\cdot 2H_2O$, **3**:$(QUIN^{+})\cdot(D\text{-}MA^{-})\cdot H_2O$ and **4**: $2(QUIN^{+})\cdot((0.75\,D\text{-}MA^{2-})\cdot(0.25\,L\text{-}MA^{2-}))\cdot 2H_2O$ (Scheme 1).

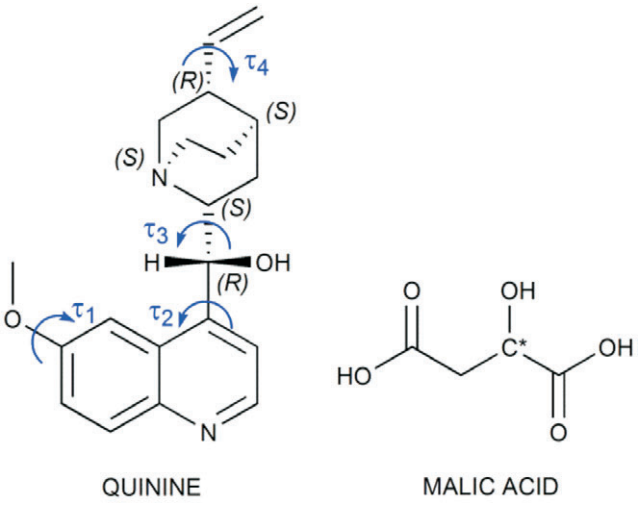

Scheme 1
Stereo descriptors of quinine with the measured torsion angles and the molecular structure of malic acid.

2. Experimental Details

2.1. Crystal Growth

All chemicals were purchased from commercial sources (Sigma-Aldrich) and used without further purification. Compounds **1**, **2** and **4** were prepared by mixing quinine (100 mg, 0.3 mmol) with the appropriate acid (20 mg, 0.15 mmol) in the stoichiometric ratio of 2:1 using 96 % ethanol as solvent. Needle-shaped crystals were obtained by slow evaporation after one week. Compound **3** was prepared by mixing quinine with *D*-malic acid in 2:1 ratio in water. Slow evaporation yielded block like crystals after a week.

2.2. Structure Analysis

Intensity data of a selected single crystal was collected on a Bruker DUO APEX II diffractometer[21] with graphite monochromated Mo-Kα1 radiation (λ = 0.71073 Å) at 173 K using an Oxford Cryostream 700. Data reduction and cell refinement were performed using SAINT-Plus.[22] The space group was determined from systematic absences by XPREP.[23] The structure was solved using SHELXS-97[24] and refined using full matrix least squares methods in SHELXL-97[21] with the aid of the program X-Seed.[25] The hydrogen atoms bound to carbon atoms were placed at idealized positions and refined as riding atoms with *U*iso (H) = 1.2 *U*eq (Ar-H, CH_2) or 1.5 *U*eq (CH_3). The refinement of the hydroxyl hydrogen and hydrogens of the nitrogen atoms was carried out by first locating them on a difference electron density map and subsequently imposing an appropriate bond length constraint. Diagrams and publication material were generated using PLATON,[26] X-Seed and Mercury (3.1).[27] Crystal data and structure refinement parameters are given in Table 1. CCDC 928754–928757 contain the supplementary crystallographic data for structures **1–4**. These data can be obtained free of charge *via* www.ccdc.cam.ac.uk/data_request/cif, by e-mailing data_request@ccdc.cam.ac.uk, or by contacting the Cambridge Crystallographic Data Centre, 12 Union Road, Cambridge CB2 1EZ, UK; fax: +44(0)1223-336033.

3. Results

3.1. Structures

Compound **1** crystallizes in the space group *C*2 with Z = 2. The chiral carbon C9 of quinine is known to have (*R*)-configuration and it was assigned accordingly. Protons from each carboxylic acid moiety have been transferred to the quinuclidine nitrogens (N11) of quinine, yielding a salt of stoichiometry $2(QUIN^{+})\cdot(L\text{-}MA^{2-})\cdot 2H_2O$. The malate anion is located on a diad at Wyckoff position *b* and therefore the hydroxyl group has site occupancy of 0.5. The packing of the quininium cations, the

Table 1 Crystal data for **1–4**.

Compound	**1** $2(QUIN^{+})\cdot(L\text{-}MA^{2-})\cdot 2H_2O$	**2** $2(QUIN^{+})\cdot(D\text{-}MA^{2-})\cdot 2H_2O$	**3** $(QUIN^{+})\cdot(D\text{-}MA^{-})\cdot H_2O$	**4** $2(QUIN^{+})\cdot(D\text{-}MA^{2-})\cdot 2H_2O$
CCDC No.	928754	928755	928756	928757
M_r	408.97	408.97	476.52	408.97
Temperature/K	173(2)	173(2)	173(2)	173(2)
Crystal size/mm^3	0.20 × 0.20 × 0.15	0.15 × 0.15 × 0.10	0.25 × 0.25 × 0.20	0.10 × 0.10 × 0.10
Crystal system	Monoclinic	Monoclinic	Monoclinic	Monoclinic
Space group	*C*2 (No.5)	*C*2 (No.5)	*C*2 (No.5)	*C*2 (No.5)
a/Å	20.5669(18)	20.5373(18)	20.395(3)	20.513(3)
b/Å	6.6376(6)	6.7424(6)	6.8096(9)	6.6802(8)
c/Å	15.5538(15)	15.5061(14)	19.904(3)	15.5242(19)
α/deg	90	90	90	90
β/deg	103.906(2)	105.843(2)	122.357(2)	104.991(3)
γ/deg	90	90	90	90
V/Å^3	2061.1(3)	2065.6(3)	2335.2(5)	2054.9(5)
Z	2	2	4	2
ρ(calcd)/Mg m^{-3}	1.318	1.315	1.355	1.315
μ(Mo-K$_\alpha$)/mm^{-1}	0.095	0.095	0.102	0.095
Theta range for data collection/deg	2.04, 25.70	2.06, 26.41	1.21, 29.11	2.06, 30.61
Reflections collected	3484	5405	15413	6983
No. unique data	3125	3780	5804	5529
No. data with I > 2σ(I)	2900	3290	5214	4433
No. parameters	284	284	308	287
final R (I > 2σ(I))/wR_2	0.0393/0.0984	0.0738/0.1863	0.0370/0.0935	0.0689/0.231

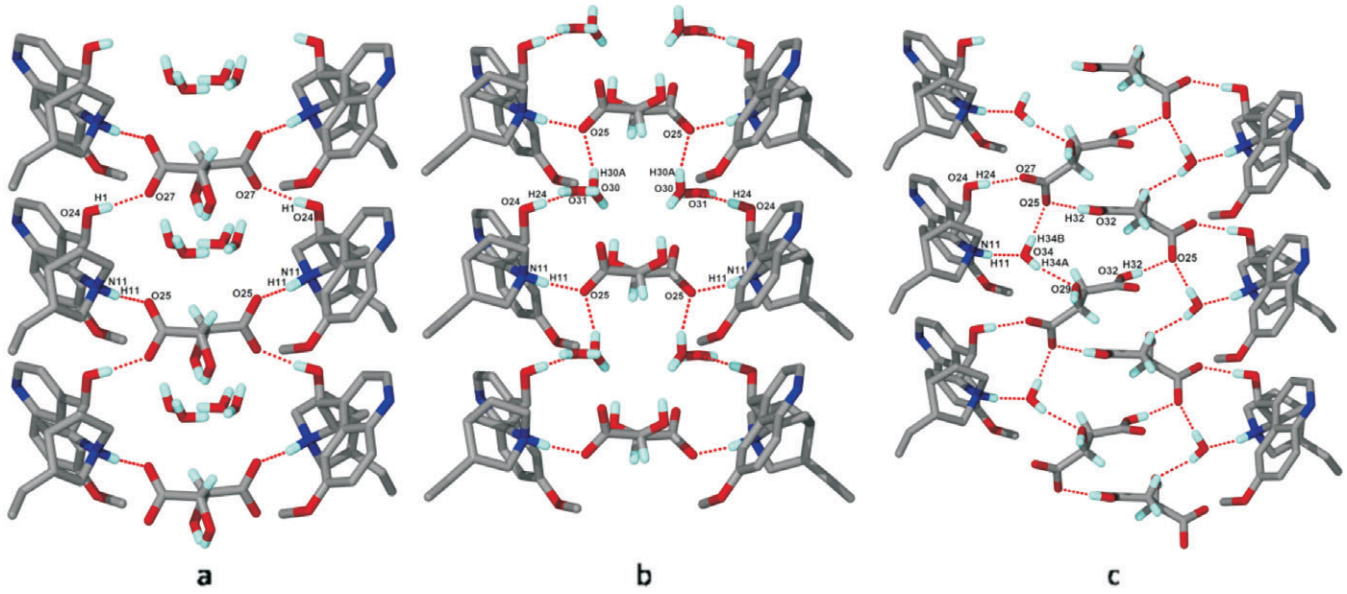

Figure 1 Packing and hydrogen bonding in structures **1** (a), **2** (b) and **3** (c).

malate anions and the disordered water molecules are shown in Fig. 1a. The hydrogen bond structure forms a ring comprising (QUIN)NH$^+$...$^-$OOC(*L*-MA)COO$^-$...$^+$HN(QUIN)OH...$^-$OOC(*L*-MA)COO$^-$ and may be described with the graph set[28] as $R_4^4(25)$. The metrics of the hydrogen bonding for this and the other structures are given in Table 2.

Structure **2** is similar to **1**, in that it also crystallizes in *C*2 with Z = 2 and the malate anion is again located on a diad and displays similar hydrogen bonds. The only difference occurs in the packing of **2** which is displayed in Fig. 1b. The hydrogen bonding forms a large ring structure comprising (QUIN)NH$^+$...$^-$OOC(*D*-MA)COO$^-$...$^+$HN(QUIN)OH...H_2O...–OOC(*D*-MA)COO$^-$...H_2O... HO(QUIN$^+$). The water is disordered over two positions and modelled with half site occupancies. The hydrogen bond pattern may be described as $R_6^6(30)$.

Structure **3** has a different stoichiometry in that the cation:anion ratio is 1:1 and this may be explained by the crystallization conditions. Quinine solubility is very good in alcohols (1 g dissolves in 0.8 mL alcohol[29]) but drastically less in water (1 g dissolves in 1900 mL water). Malic acid solubility is only slightly higher in alcohols (86.60 g 100 g^{-1} ethanol) than in water (36.35 g 100 g^{-1} water). Therefore changing the crystallization solvent from ethanol to water has significant effect on the stoichiometric ratio of the crystal. The structure again crystallizes in *C*2 with Z = 4 and all moieties lie in general positions. The water is ordered and bridging between the quininium and the malate moieties

Table 2 Hydrogen bond metrics for **1–4**.

D-H...A	D-H/Å	H...A/Å	D...A/Å	D-H...A/°	*Symmetry operator
1					
O24 – H1...O27*	0.84	1.83	2.665(0)	172	1/2-x,1/2+y,1-z
N11 – H11...O25*	0.99	1.72	2.703(9)	171	1/2-x,-1/2+y,1-z
O29 – H29...O30	0.84	2.07	2.847(8)	153	
O29 – H29...O31	0.84	2.05	2.410(6)	105	
O30 – H30B...O27	0.85	2.31	2.988(8)	137	
O31 – H31A...O29	0.85	2.12	2.410(6)	103	
O31 – H31A...O29	0.85	2.12	2.410(6)	100	
O31 – H31B...O27	0.84	2.28	2.814(3)	121	
2					
N11 – H11...O25*	0.94	1.79	2.724(5)	172	1/2-x,-1/2+y,1-z
O24 – H24...O30*	0.84	2.21	3.035(2)	169	1/2-x,1/2+y,1-z
O24 – H24...O31*	0.84	1.72	2.535(9)	163	1/2-x,1/2+y,1-z
O30 – H30A...O25	0.85	2.01	2.631(9)	130	
3					
N11 – H11...O34	0.91	1.90	2.801(2)	171	
O24 – H24...O27*	0.89	1.87	2.760(2)	170	x,-1+y,z
O29 – H29...O27*	0.91	1.86	2.763(7)	170	-x,y,-z
O32 – H32...O25*	0.88	1.84	2.704(5)	169	1/2-x,-1/2+y,-z
O34 – H34A...O27	0.78	2.59	3.089(4)	124	
O34 – H34A...O29	0.78	2.17	2.929(9)	167	
O34 – H34B...O25*	0.85	1.89	2.732(9)	175	x,-1+y,z
4					
N11 – H11...O27*	0.93	1.82	2.743(5)	175	1/2-x,1/2+y,-z
O24 – H24...O30*	0.84	1.79	2.583(4)	177	x,1+y,z
O30 – H30A...O25	0.85	2.28	2.611(5)	143	

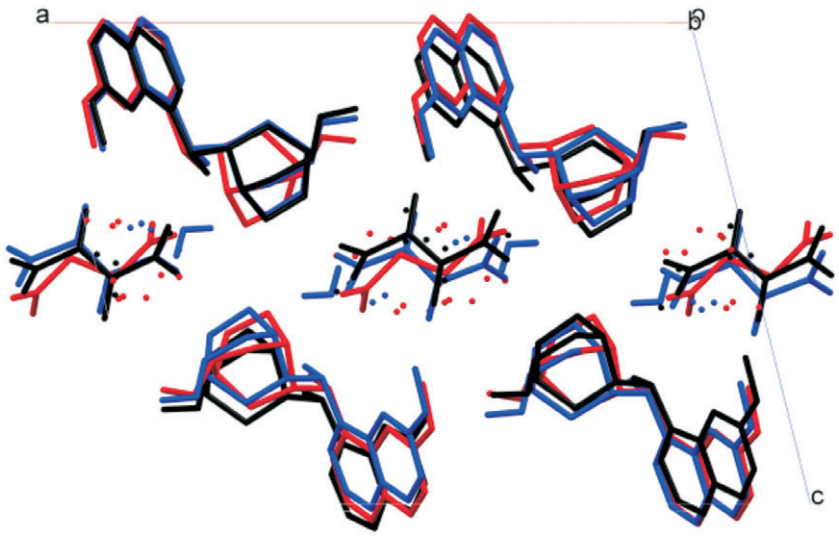

Figure 2 Isostructurality of **1** (red), **2** (blue) and **4** (black). The quininium cations form a framework with channels running along [010].

(Fig. 1c). The hydrogen bonding comprises a ring (QUIN)NH^+...H_2O...$^-$OOC(*D*-MA)COOH...$^-$OOC(*D*-MA)COOH...$^-$OOC(*D*-MA)...HO(QUIN$^+$) and can be described as $R_5^5(25)$.

Structure **4** was obtained by exposing QUIN to *DL*-malic acid. The QUIN partially resolved the racemic mixture and the resultant crystals yielded the malate salt with *D:L* in the ratio of 75:25. Therefore compound **4** has the formula 2(QUIN$^+$)·((0.75 *D*-MA^{2-})·(0.25 *L*-MA^{2-}))·2H_2O. The structure is similar to **2**, with the exception of the water of crystallization being ordered. The hydrogen bonding with the major component is as described for **2**.

Structures **1**, **2** and **4** are essentially isostructural, in that the quininium cations form a framework with channels which contain diads running along [010]. These channels accommodate the malate anions which are therefore disordered and also some water molecules. In structures **1** and **2** different positions are adopted by the *L*- or *D*-malate anions, but they share a common position for the O atom that is a hydrogen bond acceptor from the quininium cation. (Fig. 2.) The nature of the disorder in **4** is clear hence the channels are inherently 2-fold symmetric.

3.2. Thermoanalysis

The thermogravimetric (TG) and the differential scanning calorimetry (DSC) curves for the four compounds are very similar, therefore we show the results of **1** as being representative (Fig. 3). For all compounds, the onset and peak temperatures as well as the theoretical and measured mass losses are reported in Table 3. The TG curve shows an initial mass loss attributed to the loss of water of crystallization. The curve is then flat to *ca.* 470 K after which the salt decomposes. The concomitant

Table 3 Thermoanalytical results of **1–4**.

Compound	**1**	**2**	**3**	**4**
Cation:anion:water ratio	2:1:2	2:1:2	1:1:1	2:1:2
$Endo_1$ (T_{peak}/K)	368	385	400	343
$Endo_2$ (T_{on}/K)	458	449	452	451
% mass loss	3.8	4.3	4.5	4.4
% theoretical mass loss	4.4	4.3	3.8	4.4

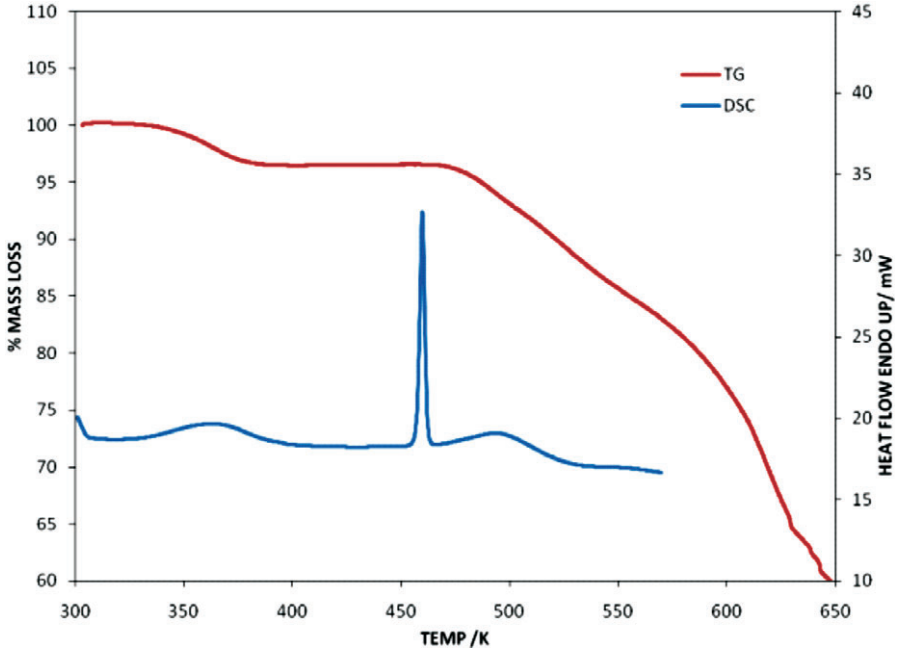

Figure 3 TG and DSC curves of **1**.

DSC curve exhibits an initial endotherm corresponding to the loss of H_2O, followed by a sharp peak due to the melt of the salt. There is good agreement between experimental and theoretical mass losses. Because the loss of water gives rise to a broad endotherm, we report the peak and not the onset temperatures.

3.3. Conformation Analysis

We have recorded the four torsion angles τ1 (C5-C6-O22-C23), τ2 (C3-C4-C9-O24), τ3 (O24-C9-C10-N11) and τ4 (C14-C13-C18-C19) which define the conformation of quinine. (Scheme 1, Table 4) We have compared our findings to the search conducted on the published quinine structures in the CSD. The torsion angles of the 26 structures (overall 40 hits) are shown in Table 5. The polar histograms of the search results and the torsion angles of the four currently reported structures are shown in Fig. 4. We note that τ1, τ2 and τ3 are remarkably constant. The torsion angles of the four new structures are marked as red arrows on the perimeters and they fit the trends shown on the polar histograms.

Table 4 Relevant torsion angles in **1–4**.

Compound	**1**	**2**	**3**	**4**
τ1(°)	–0.1 °	0.64 °	–2.35 °	–0.04 °
τ2(°)	–15.9 °	–16.22 °	–18.35 °	–17.32 °
τ3(°)	–80.95 °	–74.80 °	–80.20 °	–75.72 °
τ4(°)	–131.04 °	–116.60 °	–130.54 °	–115.79 °

However, some structures do not fit the trend. In the structures of YUKMOG (diquininium (fluoro(hydroxyphenyl-phosphinyl)-methyl)phosphonate acetone solvate sesquihydrate[30]) and XUNZIQ (6′,9-dihydroxycinchonan-1,1′-diium hexachlorobismuthate chloride monohydrate[31]) there are two symmetry independent quininium cations in the asymmetric unit and in one of them the methoxy group related to τ1 occupies the conformation at t ~180 ° (Fig. 4a).

The distribution of τ2 shows one structure (XEGTAF: β-cyclodextrin (6-methoxyquinolin-4-yl) (5-vinyl-1-azabicyclo[2.2.2] oct-2-yl)methanol clathrate hydrate[32]) where the hydroxyl group of the quinine is nearly perpendicular to the quinoline ring. (Fig. 4b) Also XEGTAF shows significant difference in τ3. (Fig. 4c) It is interesting to note that in this structure the quinuclidine moiety is included in a β-cyclodextrin and the authors suggested that this is the reason for its exceptional conformation. The distribution of τ4 suggests that in the majority of the structures the torsion angle of the ethylene moiety centred around –118 °. However, 13 structures show remarkable differences. 12 are clustered between 111–157 ° and in one (XUNZIQ) τ4 is –166 °. (Fig. 4d) It is noteworthy that the flexibility of the ethylene moiety has been connected to the chiral selectivity of quinine in diastereomeric salt formation with mandelic acid (UYEZII, UYEZOO, UYEZOO1 and UYIBAG[17]) These diastereomeric pairs do not show any significant difference in any of the four torsion angles but it was concluded that the resolution of mandelic acid by quinine is driven by intermolecular hydrogen bonds and slight concomitant changes in the τ4 torsion angle.

3.4. Hirshfeld Surface Analysis

The precise mechanism of chiral discrimination is still unknown. Very few solid state studies have been carried out to date; however, there are some current attempts to investigate the process in solution *via* combining theoretical and experimental studies.[34] In agreement all these works point out the importance of the non-bonded interactions, particularly the hydrogen bonds in the discrimination process.

Table 5 Quinine torsion angles in structures deposited to CSD. The exceptions are given in bold.

No.	CSD code	τ1(°)	τ2(°)	τ3(°)	τ4(°)
1	BEYTIJ	2	–21	–80	–108
2	**ELIPAQ**	–6	–27	–73	**133**
	ELIPAQ	–4	–23	–77	–102
3	**FEQZEG**	0	-13	–85	**157**
4	FIJSUM	3	–15	–82	–119
5	IROQEL	0	–19	–73	–110
6	**JIFYOM**	10	–24	–76	**124**
	JIFYOM	8	–25	–74	–131
7	KAMDAD	8	–14	–90	–111
8	KURPET	–4	–25	–76	–120
9	LIVWOC	–1	–22	–76	–117
10	PUVTUV	–1	–25	–77	–111
	PUVTUV	1	–21	–78	–123
11	ROHJAZ	–3	–24	–84	–124
12	**UMUPIB**	–3	–9	**–53**	**147**
13	**URIYAW**	–2	–14	–61	**136**
	URIYAW	1	–14	–57	**117**
14	VAZCUV	–4	–29	–83	–116
15	WANTOU	1	–12	–80	–123
16	**XEGTAF**	–6	**–99**	**–171**	–116
17	**XUNZIQ**	10	–3	–60	**–166**
	XUNZIQ	**170**	–13	–62	**132**
18	YANNIL	5	–14	–75	–106
19	YUCXIE	0	–22	–73	–110
20	YUKMOG	4	–21	–74	–122
	YUKMOG	**–145**	–22	–64	121
21	ZZZMNO01	0	–16	–78	–123
22	ROHJAZ01	–4	–24	–84	–124
23	**UYEZII**	–8	–17	–77	**111**
	UYEZII	–6	–23	–81	–103
	UYEZII	–2	–13	–75	–118
24	**UYEZOO**	–8	–17	–77	**116**
	UYEZOO	–6	–23	–80	–105
	UYEZOO	–2	–13	–75	–118
25	**UYEZOO01**	–7	–16	–77	**117**
	UYEZOO01	–7	–23	–81	–106
	UYEZOO01	–3	–13	–75	–117
26	**UYIBAG**	–6	–21	–80	**121**
	UYIBAG	–9	–17	–78	–111
	UYIBAG	–7	–12	–71	–111

In order to understand the mechanism of resolution of the *DL*-malic acid by QUIN, we analyzed the non-bonded interactions which occur in the hydrated $(QUIN^+)(MA^-)\cdot$salts. We employed the program Crystal Explorer[35] which calculates the Hirshfeld surfaces of a molecule or ion in a crystal structure and depicts all the molecular interactions of the targeted moiety with its neighbours in the form of fingerprint plots.

In Fig. 5a the fingerprint plots for the malate anion is shown. The spike labelled ① is associated with the hydrogen bonds $(QUIN^+)$N11-H11...O25(*L*-MA^-) and $(QUIN^+)$-OH...O27(*L*-MA^-) which contribute 58 % to the overall interactions towards the procrystal. The spike labelled ② is due to (*L*-MA-)O29- H29...O30/O31 (disordered water). The area between these two spikes is populated by H...H interactions (28 %).

In Fig. 5b, spike ① is derived from a combination of $(QUIN^+)$ N11-H11...O25(*D*-MA^-), the disordered water O30-H30...

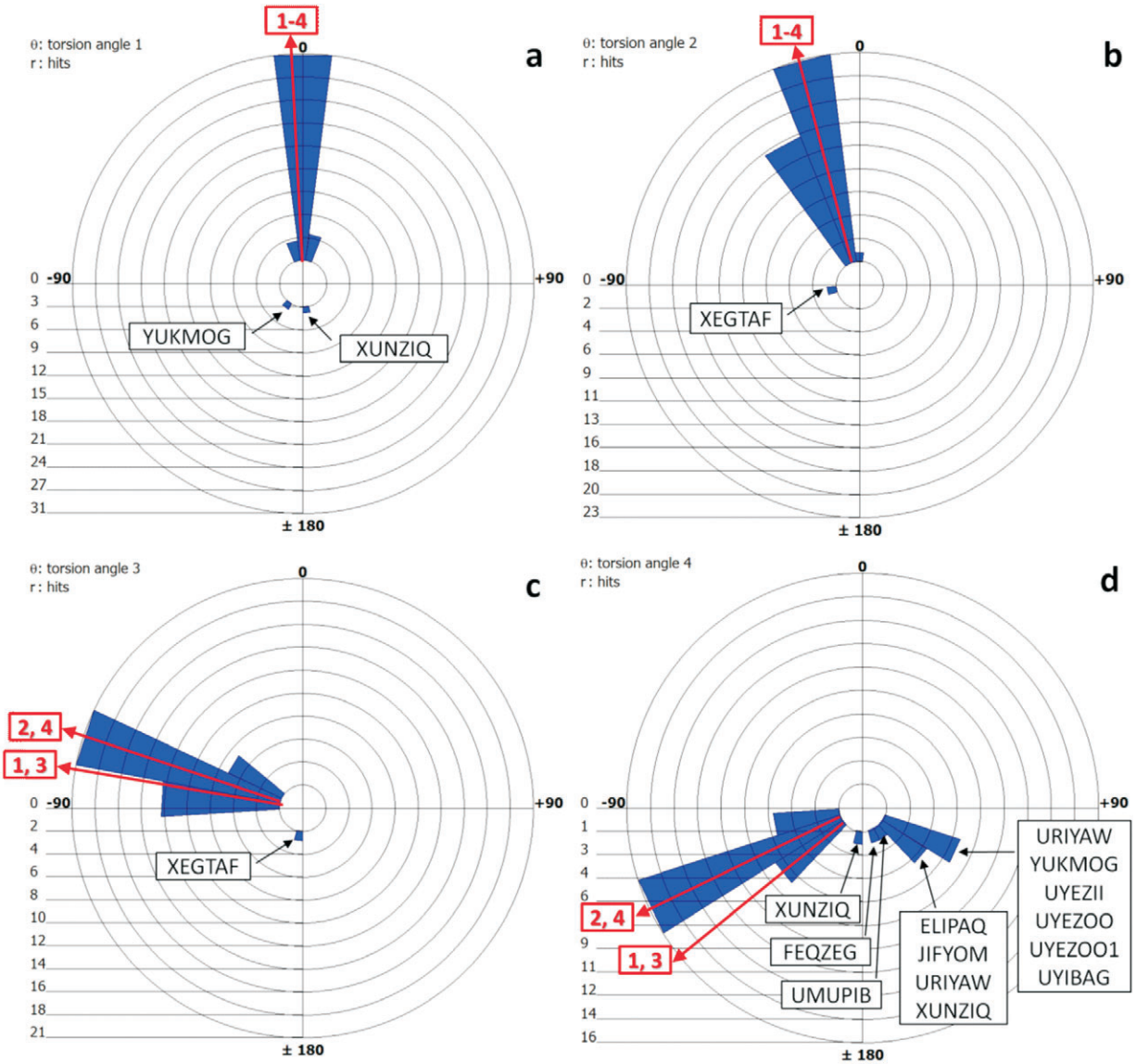

Figure 4 The distribution of the torsion angles (**a**: τ1, **b**: τ2, **c**: τ3, **d** τ4) of the quinine moiety in the crystal structures extracted from the CSD.

O25(*D*-MA$^-$), and (QUIN$^+$)C12-H12B...O27(*D*-MA$^-$) with a total contribution of 62 %. Spike ② is due to H...H interactions between MA$^-$ and the methoxy hydrogens on QUIN$^+$ (27 %).

The fingerprint of the malate anion in **3** is distinctly different and exhibits two symmetrical sharp and a broad spike between them (Fig. 5c). ① is associated with (*D*-MA$^-$)O32-H32... O25(*D*-MA$^-$) and (water) O34-H34B...O25(*D*-MA$^-$) and contribute to the overall interactions with 53 %. ② is due to (*D*-MA$^-$) O32-H32...O25(*D*-MA$^-$) and (*D*-MA$^-$)O29-H29... O27(*D*-MA$^-$) (9.6 %). Spike ③ is due to H...H interactions (31.7 %).

The major component of the malate anion in structure **4** is very similar to that of **2**, the only difference being that in **4** the water of crystallization is ordered. The fingerprint pattern of the major component of **4** resembles that of **2** closely and is distinct from that of **1**.

The resolution experiment with quinine yielded the *D*-malate

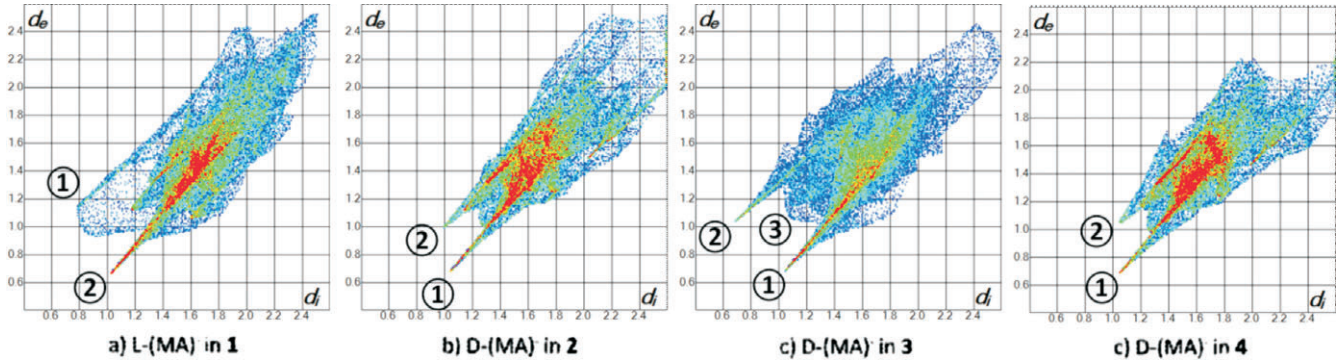

Figure 5 Fingerprint plots of the malate ions in the relevant crystals. (**a**) *L*-malate in structure **1**, (**b**) *D*-malate in structure **2**, (**c**) *D*-malate in structure **3** and (d) *D*-malate in structure **4**.

salt as the major component and one notes that the hydrogen bonding in this structure is more favourable as it involves the water of crystallization while in **1** the water is not hydrogen bonded. (Fig. 1a and Fig. 1b) This is indeed reflected in the difference and % contributions exhibited by the fingerprint plots.

4. Conclusions

The crystallization of quinine with racemic malic acid yielded the crystals of the *D*-malate salt as the major component with the QUIN:MA ratio of 1:0.5 (structure **4**). The structures of the quininium-*L*- and *D*-malate presented the same quininium: malate ratio (structures **1** and **2,** respectively). In structure **3**, quinine crystallizes with *D*-malic acid with a different stoichiometry, the QUIN:MA ratio is 1:1. The conformation of the quinine moiety in each structure was compared to the 26 known structures of quinine obtained from the CSD and showed no significant differences. The *D*-malate is the major product because its structure has a more favorable hydrogen bond pattern.

Supplementary Material

Details to download the X-ray data of the four compounds are provided in the experimental section.

Acknowledgements

Authors thank for Prof. Andrew D. Bond for his valuable comments on the manuscript and the National Research Foundation (Pretoria) and the Cape Peninsula University of Technology for financial support. The authors declare that they have no conflict of interest.

References

1 S.C. Stinson, *CENEAR*, 2000, **78**, 55–78.

2 (a) R.M. Kellogg, J.W. Nieuwenhuijzen, K. Pouwer, T.R. Vries, Q.B. Broxterman, R.F.P. Grimbergen, B. Kaptein, R. M. La Crois, E. de Wever, K. Zwaagstra and A. C. van der Laan, *Synthesis,* 2003, **10**, 1626–1638 (b) Facts and Figures, *Int. Fed. Pharm. Man. & Assoc*., 2012, http://www.ifpma.org/

3 (a) S.H. Wilen(1971) *Resolving Agents and Resolution in Organic Chemistry – Topics in Stereochemistry*, Wiley–Interscience, New York, USA, 1971, **6**, 107–176. (b) J. Jacques, A. Collet, S.H. Wilen, *Enantiomers, Racemates and Resolutions*, Krieger Publishing Company Malabar, FL., 1991 (c) F. Toda, ed., *Enantiomer Separation. Fundamentals and Practical Methods*, Kluwer Norwell, MA. 2004.

4 L. Pasteur, *C. R. Acad. Sci.,* 1853, **37**, 162–166.

5 D. Kozma, ed., *Optical Resolutions via Diastereomeric Salt Formation*, CRC Press, New York, 2002.

6 F.H. Allen, *Acta Cryst.,* 2002, **B58**, 380–388.

7 I.J. Bruno, J.C. Cole, P.R. Edgington, M. Kessler, C.F. Macrae, P. McCabe, J. Pearson and R. Taylor, *Acta Cryst*., 2002, **B58**, 389–397.

8 (a) B. Pniewska and A. Suszko-Purzycka, *Acta Cryst.,* 1989, **C45,** 638–642. (b) G. Paliwoda, B.J. Oleksyn, J. Sliwinski, *Enantiomer*, 2002, **7**, 387–396.

9 (a) B. Oleksyn and P. Serda, *Acta Cryst.,* 1993, **B49**, 530–535. (b) P. M. Bhatt, N.V. Ravindra, R. Banerjee and G.R. Desiraju, *Chem. Commun.,* 2005, 1073–1075.

10 (a) P.J.F. Griffiths, *Acta Cryst.,* 1959, **12**, 418–419. (b) P.M. Kimpede and L. Van Meervelt, *Acta Cryst.,* 2010, **E66,** o2443-o2444. (c) M. Kubicki, T. Borowiak, M. Gawron, M. Giel, J. Gawronski, *J. Crystallogr. Spectrosc. Res.,* 1990, **20**, 447–455. (d) A. Gjerlov and S. Larsen, *Acta Cryst*., 1997, **C53**, 1505–1508. (e) C. Ryttersgaard and S. Larsen, *Acta Cryst*., 1998, **C54**, 1698–1701. (f) C. Ryttersgaard and S. Larsen, *Acta Cryst*., 2004, **E60**, o4–o5. (g) B. Samas, A. C. Blackburn and K. C. Kreuchauf, *Acta Cryst*., 2005, **E61**, o3983–o3984.

11 D.H. Appella, L.A. Christianson, I.L. Karle, D.R. Powell, S.H. Gellman, *J. Am. Chem. Soc*., 1999, **121**, 6206–6212.

12 D.W. Graham, W.T. Ashton, L. Barash, J.E. Brown, R.D. Brown, L.F. Canning, A. Chen, J.P. Springer and E.F. Rogers, *J. Med. Chem.,* 1987, **30**, 1074–1090.

13 R. Bau, P.-T.T. Pham, G.D. Duncan, C.E. McKenna, *J. Med. Chem*., 1995, **38**, 1575–1578.

14 W. Tochtermann, T. Panitzsch, M. Petroll, T. Habeck, A. Schlenger, C. Wolff, E.-M. Peters, K. Peters, H.G. von Schnering, *Eur. J.Org. Chem*., 1998, 2651–2657.

15 B. Dominguez, A. Zanotti-Gerosa, W. Hems, *Org. Lett*., 2004, **12**, 1927–1930.

16 A. Jacobs, L.R. Nassimbeni, A. Sayed and E. Weber, *J. Chem. Cryst.,* 2011, **41**, 854–857.

17 N.B. Báthori, L.R. Nassimbeni and C.L. Oliver, *Chem. Commun.,* 2011, **47**, 2670–2672.

18 FAO Nutrition Meetings Report Series, No. 40, A, B, C, WHOLE/ Food Ad./67.89

19 P.P. Toffoli, N. Rodier, R. Ceolin, F. Lepage, J. Astoin, *Acta Cryst.,* 1988, **C44**, 2128–2131.

20 D.E.Turkington, G. Ferguson, A.J. Lough, C. Glidewell, *Acta Cryst.,* 2004, **C60**, o617-o622.

21 Bruker 2005. APEX2. Version 1.0–27. Bruker AXS Inc., Madison, Wisconsin, USA.

22 Bruker 2004. SAINT-Plus (including XPREP). Version 7.12. Bruker AXS Inc., Madison, Wisconsin, USA.

23 Bruker 2003, XPREP2. Version 6.14. Bruker AXS Inc., Madison, Wisconsin, USA.

24 G.M. Sheldrick, SHELXS-97 and SHELXL-97 Programs for crystal structure determination and refinement. University of Göttingen, 1997.

25 L.J. Barbour, *J. Supramol. Chem*., 2001, **1**, 189–191.

26 A.L. Spek, *PLATON, A Multipurpose Crystallographic Tool*, Utrecht University, Utrecht, Netherlands, 2008.

27 C.F. Macrae, I.J. Bruno, J.A Chisholm, P.R. Edgington, P. McCabe, E. Pidcock, L. Rodriguez-Monge, R. Taylor, J. van de Streek, P.A Wood, *J. Appl. Cryst.,* 2008, **41,** 466–470.

28 M.C. Etter, J.C. MacDonald, J. Bernstein, *Acta Cryst*., 1990, **B46**, 256–262.

29 M.J. O'Neil, ed., *The Merck Index – An Encyclopedia of Chemicals, Drugs and Biologicals*, 2006, Merck and Co. Inc., Whitehouse Station, NJ, USA.

30 R. Bau, P.-T.T. Pham, G.D. Duncan, C.E. McKenna, *J. Med. Chem*., 1995, **38**, 1575–1578.

31 H.L.Cai, T. Zhang, L.Z. Chen, R.G. Xiong, *J. Mater. Chem.,* 2010, **20**, 1868–1870.

32 Z. Fan, C.H. Diao, H.B. Song, Z.L. Jing, M. Yu, X. Chen, M.J. Guo, *J. Org. Chem.* 2006, **71**, 1244–1246.

33 (a) N.B. Báthori, L.R. Nassimbeni, *Cryst. Growth and Design*, 2010, **4**, 1782–1787. (b) N.B. Báthori, L.R. Nassimbeni, *Cryst. Growth and Design*, 2012, **12**, 2501–2507. (c) A. Bialonska, Z. Ciunik, *Cryst. Growth and Design,* 2013, **13**, 111–120.

34 R. Arjumand, I.I. Ebralidze, M. Ashtari, J. Stryuk, N.M. Cann and J.H. Horton, *J. Phys Chem. C*, 2013, **117**, 4131–4140. (b) X.-H. Zhang, H.-L. Wu, X.-L. Yin, L.-H. Li, J-Y. Wang, Y. Chen, C. Kang, R.-Q. Yu, *Anal. Methods*, 2013, **5**, 710–717.

35 (a) J.J. McKinnon, M.A. Spackman and A.S. Mitchell, *Acta Crystallogr.*, 2004, **B60**, 627–668; (b) M.A. Spackman and J.J. McKinnon, *CrystEngComm*, 2002, **4**, 378–392.